

# Design for Low Beam Loss in Accelerators for Intense Neutron Source Applications

Robert A. Jameson  
Accelerator Technology Division  
Los Alamos National Laboratory, Los Alamos, NM 87545

## Abstract

Control of beam loss in intense ion linacs involves keeping beam spill below parts in  $10^{-5}$ - $10^{-8}$ /m by preventing total beam size from extending to the limiting apertures. Starting from good rms design practices, new analysis of the machine architecture is described in terms of space-charge effects on the machine tune, free-energy constraint, and halo-producing mechanisms. It is shown that halos are produced by the time- (or position-) varying nature of common linac aspects (such as misalignment, mismatching, acceleration, and construction techniques) through collective core/single-particle interaction dynamics plus resonances.

## I. INTRODUCTION

High-intensity neutron sources can provide solutions to society's requirements for defense and commercial radioactive actinide and fission-product waste disposal and generation of electric power without a long-term waste stream [1-2], a pulsed neutron research facility [3], production of tritium and other special materials [4], conversion of plutonium, and the development of advanced materials [5]. These neutron sources are driven by large linear accelerators, with 30-300 mA proton current at energies of 1-2 GeV and 10-100% duty factors for the applications in [1-4], and modules of up to 250 mA cw deuteron current at 40 MeV for the materials development program.

These accelerators would have up to a few hundred megawatts of beam power, a large factor above the ~1 MW capability presently available at LAMPF. However, the power extrapolation is not fundamentally difficult; a factor of ~64 would be realized if LAMPF ran cw and all the rf buckets were filled. The major challenge is to keep residual activation of the linac by stray beam loss low enough that remote manipulator maintenance is not required; i.e., average losses should not exceed present LAMPF levels, translating to a rule-of-thumb of <1 nA/GeV/m. Dealing with more particles per bunch is the main challenge of the extrapolation. Most of the proposed configurations require within 2-3 times more particles per bunch, with the maximum scenario at 4-5. Acceleration of peak currents of these magnitudes has been achieved, but attainment of the required low loss must be demonstrated.

Typically, in real linacs and in multiparticle simulations of them, a high-intensity beam will develop a diffuse outer "halo" that can contain as much as a few percent of the beam current. If this halo extends to the bore radius, particles will be scraped off. There is presently no analytical guidance to performance at such low levels, and the physics in the simulation tools is also not accurate enough. Present design practice [3-5] concentrates on controlling the transverse and longitudinal rms beam sizes in ways that insure maximum "aperture factors" (or safe stay-clear ratios of bore-to-rms-beam-radius and accelerating-bucket-to-rms-beam-length) within various constraints. Reference design work for the new

applications avoids abrupt transitions such as those that cause "hot spots" at LAMPF, and achieves rms aperture factors from 2-3 times larger than the LAMPF design. New designs, including an anticipated error budget, are checked by simulation with up to a few hundred thousand particles, and are judged satisfactory if no particles are observed to hit the bore.

The simulations do show growth of the total beam size. The intent of this paper is to discuss aspects of total beam size, the control of which is the true goal of loss minimization.

## II. ARCHITECTURE OF PRESENT DESIGNS

Two dominant features characterize the essentials of a typical RFQ accelerating section, a DTL, or a long coupled-cavity high-beta ion linac (CCL). Typically the accelerating gradient is held constant, because of rf power cost or sparking constraints. This results in rather small longitudinal focusing that decreases with energy, so the longitudinal zero-current phase advance per period decreases. The longitudinal tune depression from the beam space-charge then stays about constant with energy, typically ~0.4, a value at which the space-charge and emittance have approximately equal effect. There is phase damping with acceleration and the beam rms phase width shrinks, resulting in a larger rms longitudinal aperture factor [6].

Strong transverse focusing is relatively easy to obtain. With constant transverse focusing per unit length, the external focusing effect increases with energy as the space-charge forces weaken. The rms beam size shrinks, increasing the rms transverse aperture factor. The transverse tune depression, which may be strong (~0.4) at low energy, rapidly weakens.

In terms of the plasma period of the beam, the 1-2 GeV linac is long — of order 100 plasma periods.

The emittance and aperture factor behavior reflect the architecture, as shown in Fig. 1 for a typical 140 mA, 20-1500 MeV proton linac. In this typical simulation, the error-free linac is smoothly varying and the input beam is a mathematical, clean-edged distribution injected on-axis and rms-matched.

The tune trajectories are plotted on Hofmann's beam instability chart [7], Fig. 2, to check whether the observed growth can be explained in this way. The longitudinal/transverse rms emittance ratio stays at ~2. At 20 MeV, the trajectories are initially below the 4th-even mode thresholds and a rapid equilibration occurs in 1/4 plasma period (~1-2 tanks). The trajectory is above the 3rd-odd thresholds, and the 3rd-even is not excited because the transverse tune is not under its threshold. So the lower-order Hofmann modes do not explain the growth.

It is clear from Fig. 2 that the transverse/longitudinal energy balance (or partitioning) is not equal through most of the linac [8,9] and thus free energy is available that can be converted via nonlinear processes to size/emittance growth. A major phase of present research now in progress is to modify the machine tune so that various degrees of equipartitioning

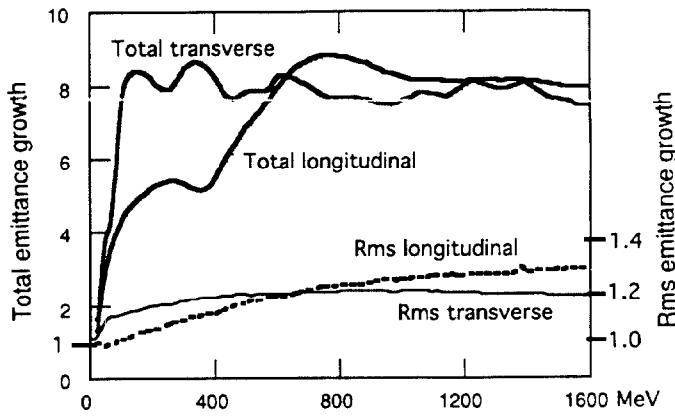


Fig. 1.a. Emittance growth in a typical CCL.

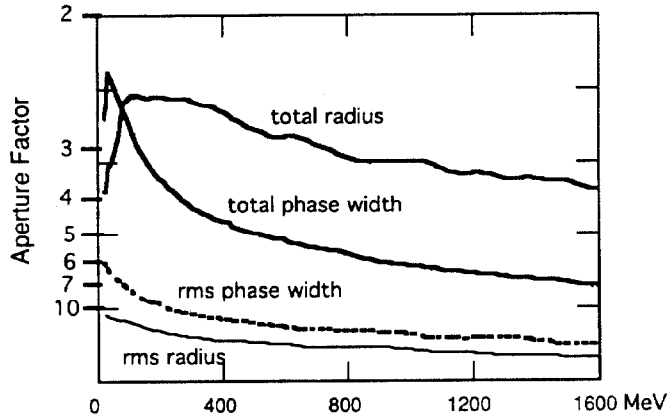


Fig. 1.b. Aperture factors in a typical CCL.

can be studied. Because the architecture economics specified the longitudinal tune, equipartitioning means a decrease in the transverse focusing with energy. Growth in rms beam size (perhaps a factor of 3-4) will occur along the machine, but if total beam size growth is reduced, an overall improvement may result. This work requires a self-consistent simulation code [8,9], which is being updated. These future studies of beam-involved machine tunes may result in a hybrid tune, with better energy balance at low energies where space-charge is more dominant, and stronger focusing at higher energies.

A superconducting (sc) linac could allow the accelerating gradient to increase with energy, allowing equipartitioning with smaller transverse beam size. This may be a major argument for sc linacs, along with larger aperture and shorter length from higher gradient.

Using the rms matching equations and the equipartitioning relationship, scaling and optimization equations for the aperture factors can be formulated [6]. Unfortunately, they are highly coupled and nonlinear and thus are not solvable except under special circumstances, such as constant equipartitioning ratios. In that case, the aperture factors are always larger at lower frequency. In other cases, optimum frequencies are evidenced in numerical studies, and some very strong relationships are indicated, such as that the maximum aperture factor always occurs at an almost constant tune depression. Some aspects of these kernel relationships have been discovered, but their basic forms remain elusive. Finding these kernels would help greatly in understanding the scaling and optimization of low beam-loss designs, so the search continues.

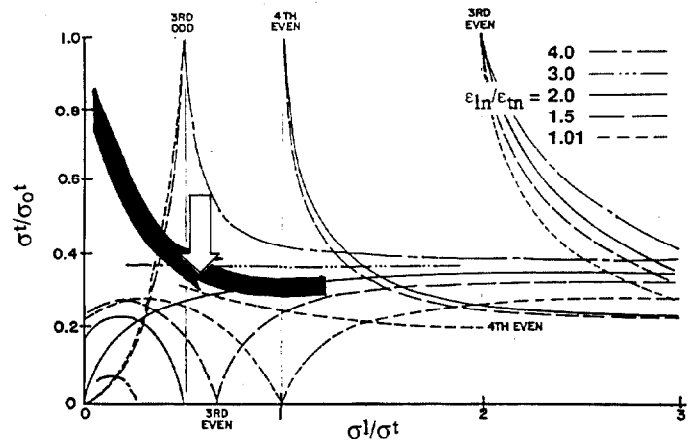
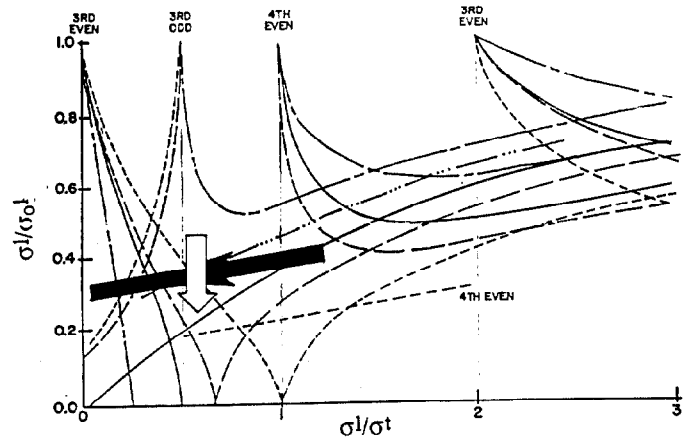


Fig. 2. CCL tune trajectories on Hofmann instability chart. Typical 140 mA, 20-1500 MeV CCL (black arrows), and equipartitioned tune (white arrows).

### III. PHYSICS OF HALO BEAMS

Preventing halo formation a priori is the point-of-view of the research thrusts of this paper. We know that this means keeping nonlinearities small in both the external fields and in the beam space-charge, keeping the beam well matched, well aligned, and energy balanced, as much as possible within the many constraints. The latter make it hard; for example, strict equipartitioning is difficult to achieve practically, especially with the need to change accelerator structure and use a higher harmonic rf at higher energy. Thus we do have to search for the mechanisms causing halo formation and how they affect allowable error budgets.

The lower-order Hofmann instability modes did not explain the results in this case. Other analyses [10-12] have related nonlinear field energy and diffusion to asymptotic rms growth (from errors of energy imbalance, misalignment, rms mismatch, and input distribution mismatch) in transport systems, but these are not easy to apply to an accelerator, and all of these methods deal in a macro-effect on the beam bunch that does not reveal what really happens to particles that may form a halo. It had long been observed that particles originally in a well-sheathed beam core could later appear in a halo, meaning that substantial energy had to be acquired by that particle, but the mechanism was not known. There were

many questions — are halos generated continuously; will they reappear if scraped; why do different error conditions produce different halo effects?

Substantial new insight has been obtained by looking at detailed single-particle behavior in computer experiments [13]. The key mechanism is very simple, and the phenomenology is elucidated in the experiments described below. Development of the corresponding theory and analytical relation to total beam size and machine tolerances is now required. As indicated schematically in Fig. 3,

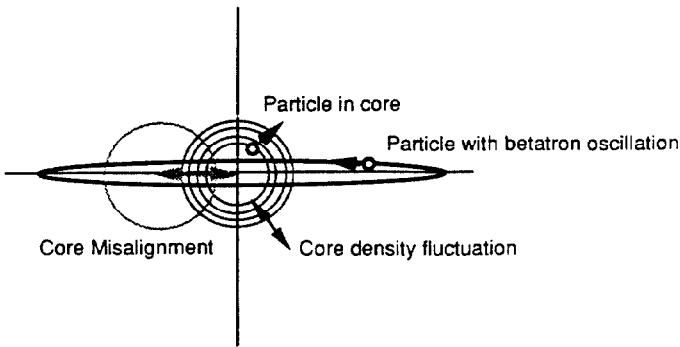


Fig. 3. Schematic of collective core/single-particle halo-producing mechanism.

the collective interaction of single particles with the beam core, when a density change in the core or a relative motion between the particle and the core occurs within an appropriate time, is a major halo-producing mechanism. Large energy transfers can occur in a single interaction; e.g., a particle with initial betatron motion can be slowed, stopped, reversed, or be accelerated by a “slingshot” effect analogous to a spacecraft passing a body in space. A particle initially at rest inside the core can receive a strong push from a nearby density

fluctuation. The accelerator is an essentially periodic system, so core fluctuations that are excited will oscillate periodically, and when a single-particle tune moves into resonance with the core oscillation, resonant interactions result in large orbits. Thus can particles move from the center of the core into the outer halo. The resonances tend to self-limit as the particle tune changes when its orbit changes. The core/single-particle interactions give a unifying insight into the halo-forming contributions of mismatching, misalignment, energy imbalance, alternating-gradient focusing, constant-beta linac sections, bunching, acceleration and other causes of beam core fluctuation. Some of the features of the mechanism are briefly summarized in the following.

The time-varying dynamics were first understood by observing the behavior of an initially round, continuous, zero-emittance, strongly mismatched,  $3\text{-}\sigma$  Gaussian beam launched into a linear continuous radial focusing channel. Fig. 4 shows its evolution. (When  $x$  or  $y$  change sign, the sign of  $r$  is reversed, and  $r'$  adjusted, to aid the eye.) At  $z/wp = 0.375$  plasma periods, some particles are still at rest near the origin. Then the outer tail sweeps through the origin, causing a local density anomaly there that repels nearby particles, and also slows or speeds up particles in the tail. This can be observed at  $z/wp = 0.5$  and subsequently. Repeated interactions of this type result in folding of segments into a beam core ( $z/wp=3.875$ ), from which new tail segments begin to emerge. By  $z/wp = 9.750$ , the new tail extends almost as far as the original tail. The result of an abrupt scraping of the halo at  $z/wp = 50$  can now be easily anticipated by considering the mechanism as described above — a strong central density oscillation is still present, so halo continues to form.

Fig. 5 shows the central density fluctuation induced by launching a warm (initial tune depression  $\sim 0.4$ ) mismatched Gaussian beam, and the  $rr'$  radius of the six particles (from a set of 10K) that had the largest  $rr'$  radii at  $z/wp = 10$ . The sharp dip in  $rr'$  indicates a passage through the core, and it

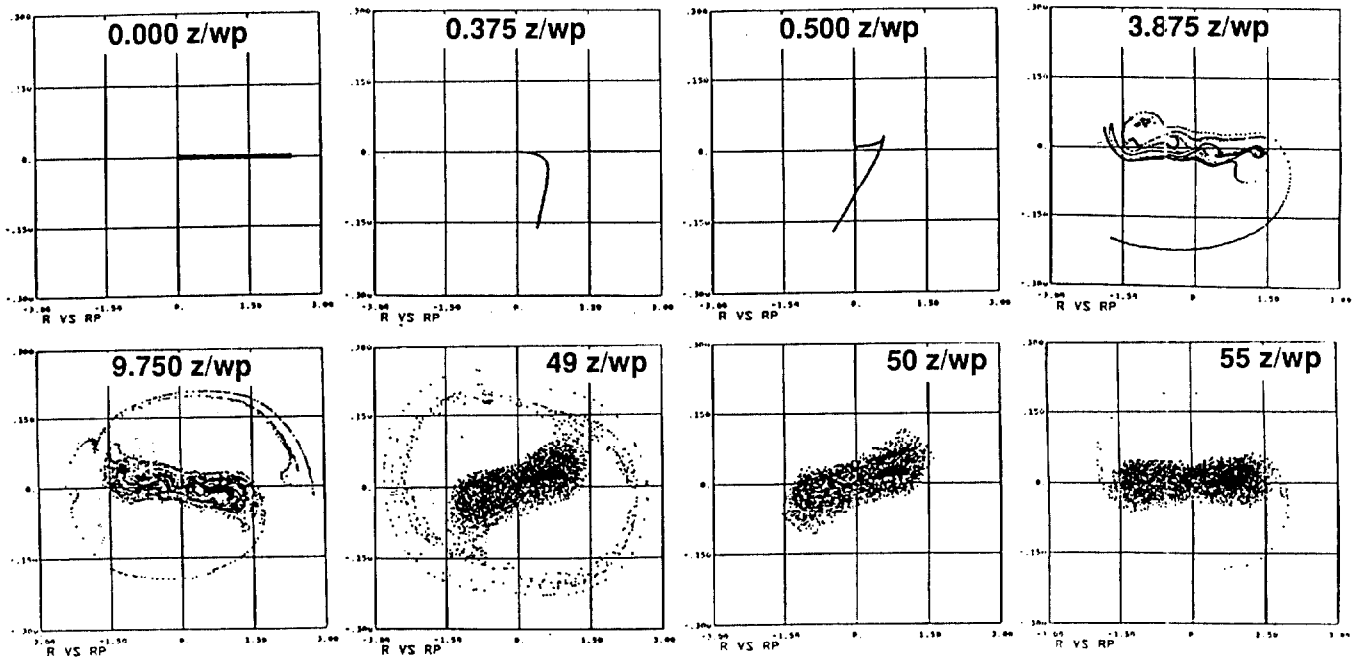


Fig. 4. Initially zero-emittance, mismatched beam in radial channel; scraped at  $z/wp = 50$ .

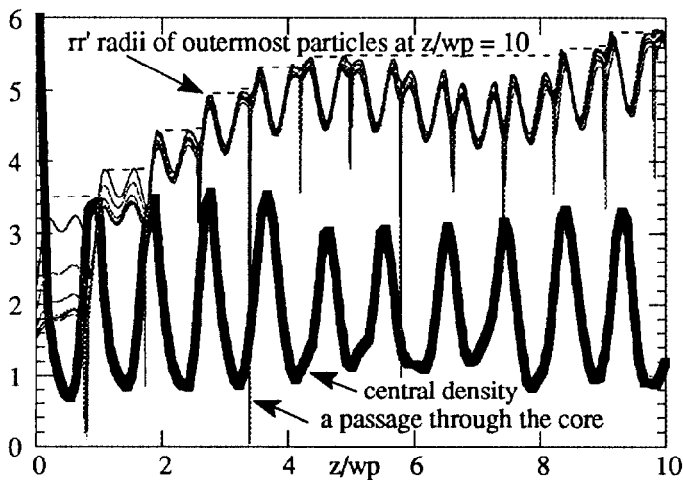


Fig. 5. Warm mismatched beam in radial channel.

will be noted that the peak in  $rr'$  following each of these interactions with the core is larger (if the interaction occurred when the central density was rising), or smaller (if the central density was falling). There is a resonant buildup during the first 5 interactions, with a change in single-particle tune that causes a slip to the falling density phase, resulting in loss of energy and change of tune back into resonant growth again at the end.

Stationary distributions can be formed [14] for the time-independent continuous radial focusing system using functions of the single-particle Hamiltonian (including space-

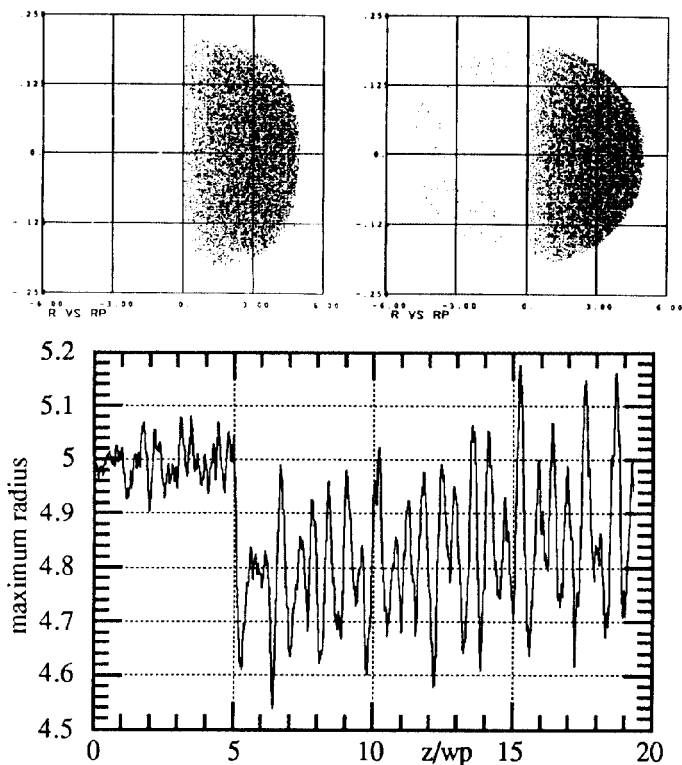


Fig. 6. (a.) Hamiltonian  $\sigma/\sigma_0 = 0.4$  initial distribution. (b.) Scraped at  $z/wp = 5$ . (c.) regrowth of maximum radius.

charge). The beam radius and focusing strength are chosen, giving the tune depression. In  $r-r'$  phase space, the distribution has a squarish shape that sharpens with more tune depression (Fig. 6.a.) An initial distribution with tune shift  $\sigma/\sigma_0 = 0.4$  was scraped with an elliptical  $rr'$  filter after 5 plasma periods (Fig. 6.b.). This excited a central density oscillation, and the maximum beam radius grew back larger than the initial value (Fig. 6.c.). As expected, the largest radius particles were driven as described above.

The stationary  $\sigma/\sigma_0 = 0.4$  distribution was given an initial mismatch of 1.5 in radius. After 20 plasma periods, rms emittance had grown only 2-3%, the maximum rms radius remained unchanged, but the maximum radius grew by a factor of  $\sim 2.4$  (times the matched radius - includes all the mismatch) via a strong resonant interaction on the rising side of the central density during the period from 8-14  $z/wp$ .

With an initial 50% beam radius misalignment (in  $x$ ) of the  $\sigma/\sigma_0 = 0.4$  Hamiltonian distribution, the rms emittance oscillated to a peak of  $\sim 15\%$  growth, damping to 3-4% at 10  $z/wp$ . The maximum radius grew about 5% beyond the shift introduced by the misalignment. Only a small oscillation was excited in the central density over this distance. There was about 20% damping of the  $x$ -centroid oscillation, with growth in the  $y$ -centroid motion. The reason for the small total growth is that there is no resonant effect because of the wide separation between the particle tunes (near 0.4) and the undepressed betatron motion of the beam centroid. We would then expect more disturbance to a beam with less tune depression, and this was indeed the case. A 50%  $x$ -misalignment of a  $\sigma/\sigma_0 = 0.83$  distribution resulted in 12% rms emittance growth over the first 6  $z/wp$ . The maximum beam radius grew 20% beyond the misalignment shift (or to 1.8 times, including the misalignment, the radius of the on-axis beam). The  $x$ -centroid oscillation (Fig. 7) damped about a factor of 10, with excitation of a central density oscillation during the strongest part of the centroid oscillation damping, that then continued at roughly constant amplitude and a frequency slightly higher than that of the decaying centroid oscillation. Fig. 7 also shows the  $rr'$  radius of the particle that was largest at  $z/wp = 10$ , achieved by resonating with the  $\sigma_0$  position-oscillation on the rising edge of  $abs(x_{mean})$  during the first 6  $z/wp$ . From 6-15  $z/wp$ , the particle's  $rr'$  radius decreases as it interacts with the admixture of centroid and central density oscillations. From 15-20  $z/wp$ , the centroid oscillation is small and the particle moves out again in resonance with the rising edge of the central density oscillation. This evidence that misalignment effects are worse for a beam with small tune depression is another reason to explore the equipartitioned tune of Fig. 2.

Energy equilibration via equipartitioning was demonstrated by injecting an unbalanced beam using the  $xx'$  distribution from a  $\sigma/\sigma_0 = 0.1$ , and  $yy'$  from a  $\sigma/\sigma_0 = 0.83$  distribution. In 10  $z/wp$ , the rms emittance growth was damping out at  $\sim 7-8\%$ , but the maximum radius growth was about 25% and still growing almost linearly. A strong central density oscillation was excited, with an increase in maximum radius on every rise in central density.

The 60-cell bunching section of a high-current RFQ was also studied [13]. In this section, the beam is at injection energy and encounters a steadily rising bunching voltage. The forming bunch makes a time-dependent density distribution.

A few (order 0.2%) particles were anomalously repelled longitudinally far from the bunch point, in some cases into the next bucket. It was found that these extraordinary orbits were

strongly correlated with very close encounters with the transverse  $xx'yy'$  origin.

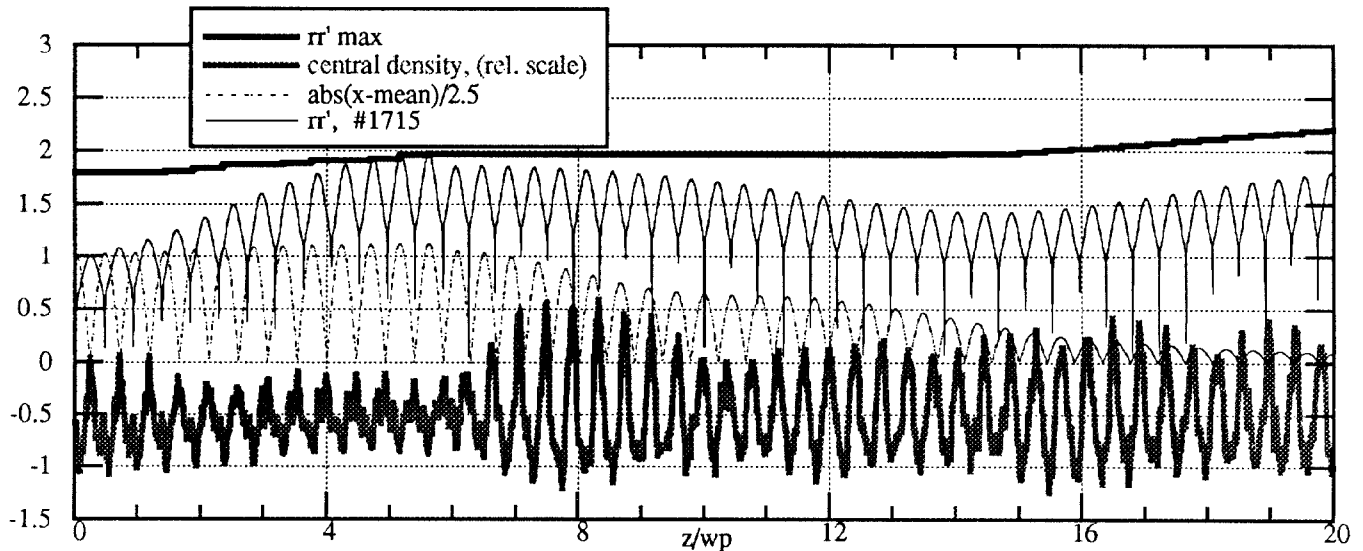


Fig. 7. Hamiltonian  $\sigma/\sigma_0=0.83$  distribution misaligned 50% of beam radius in  $x$ .

#### IV. SUMMARY

Better knowledge of how halos are actually formed gives specific rationale for modeling descriptions of total beam behavior, development of space-charge tune architecture, and scaling/optimization procedures. In future work, it is of interest to explore the features (e.g., the relative growth of core vs. halo, limiting behavior, addition of multiple errors) of each type of perturbation, plus others such as alternating gradient focusing, constant-beta sections of accelerator cells, and graded-beta acceleration – all sources of time-dependent behavior. There are many practical aspects, e.g., tune strategy regarding misalignment, determination of adequate aperture factors, and error tolerances, that need to be worked out. P. Channell has begun theoretical modeling of the core/single-particle interactions, and R. Gluckstern has sketched a model for the resonance crossing with self-limiting behavior. We must tie these together, describe the tune spread of beams under various conditions, and relate the tune spread to the various resonances and number of particles that will be excited. We hope to use this new insight into the actual halo growth mechanism to accomplish macro-modeling of the total beam size.

#### V. ACKNOWLEDGMENTS

The able assistance of G. Boicourt with the simulations is gratefully acknowledged. The studies and ideas herein are the work of the author. The evidence was presented during its evolution to stimulate theoretical development. Discussions with P. Channell and R. Gluckstern, who are now working on the theory, and C. Bohn were very stimulating.

#### VI. REFERENCES

[1] C.D. Bowman, E.D. Arthur, et. al., "Nuclear Energy Generation and Waste Transmutation Using an Accelerator-Driven Intense Thermal Neutron Source", *NIM in Phys. Res.*, (Sec. A), Vol. A320, Nos.1,2, Aug. 15, 1992, pp. 336-367.

[2] F. Venneri, C. Bowman, R. Jameson, "Accelerator-Driven Transmutation of Waste (ATW) - A New Method for Reducing the Long-Term Radioactivity of Commercial Nuclear Waste", LA-UR-93-752, Los Alamos Natl. Lab., sub. for publ. to *Physics World*, Bristol, England.

[3] A. Jason, et. al., "Los Alamos Design Study for a High Power Spallation Neutron Source Driver", these proceedings.

[4] "Accelerator Production of Tritium", *JASON* Report JSR-92-310, The Mitre Corporation, McLean, VA (1992).

[5] R.A. Jameson, "Accelerator-Driven Neutron Sources for Materials Research", *NIM in Phys. Res.* B56/57 (1991) 982-986.

[6] R.A. Jameson, "On Scaling & Optimization of High Intensity, Low-Beam-Loss RF Linacs for Neutron Source Drivers", LA-UR-92-2474, Los Alamos Natl. Lab., *Proc. 3rd Workshop on Adv. Accel. Concepts*, 14-20 June 1992, Port Jefferson, Long Island, NY, American Institute of Physics.

[7] I. Hofmann, I. Bozsik, "Computer Simulation of Longitudinal-Transverse Space Charge Effects in Bunched Beams", *1981 Linac Conf.*, LA-9234-C, Los Alamos, Natl. Lab., pp.116-119.

[8] R.A. Jameson, "Beam Intensity Limitations in Linear Accelerators", *IEEE Trans. Nucl. Sci.*, Vol. NS-28, No. 3, June 1981, pp. 2408-2412.

[9] R.A. Jameson, "Equipartitioning in Linear Accelerators", *1981 Linac Conf.*, LA-9234-C, Los Alamos, Natl. Lab., pp.125-129.

[10] T.P. Wangler, et. al., "Relation Between Field Energy and RMS Emittance in Intense Particle Beams", 1985 PAC, *IEEE Trans. Nucl. Sci.*, Vol. NS-32, No. 5, October 1985.

[11] M. Reiser, "Emittance Growth in Mismatched Charged Particle Beams", 1991 IEEE PAC, 91CH3038-7 Conf. Record, p. 2497.

[12] C.L. Bohn, "Transverse Phase-Space Dynamics of Mismatched Charged-Particle Beams", *Phys. Rev. Letters*, Vol. 70, No. 7, 15 Feb. 1993, p. 932.

[13] R.A. Jameson, "Beam Halo From Collective Core/Single-Particle Interactions", LA-UR-93-1209, Los Alamos National Laboratory, March 1993.

[14] R. Gluckstern, R. Mills, K. Crandall, "Stability of Phase Space Distributions in Two Dimensional Beams", *Proc. Linac Conf.*, National Accel. Lab. (FNAL), September 1970, p. 823.